

EXPERIMENTAL EVIDENCE FOR THE ROLE OF CROSS-RELAXATION IN PROTON NUCLEAR MAGNETIC RESONANCE SPIN LATTICE RELAXATION TIME MEASUREMENTS IN PROTEINS

BRIAN D. SYKES, WILLIAM E. HULL, AND GRAYSON H. SNYDER,
*Medical Research Council Group on Protein Structure and Function and
the Department of Biochemistry, The University of Alberta,
Edmonton, Alberta, Canada T6G 2H7*

ABSTRACT Proton nuclear magnetic resonance (NMR) spin lattice relaxation time (T_1) and spin-spin relaxation time (T_2) measurements are presented for a number of proteins with molecular weights spanning the range of 6,500–150,000 daltons. These measurements provide experimental evidence for the role of cross-relaxation in ^1H NMR T_1 measurements in proteins. The relationship between these measurements and the theory recently presented by Kalk and Berendsen is discussed. The results indicate that cross-relaxation dominates the T_1 measurements for the larger proteins, even at relatively low resonance frequencies such as 100 MHz.

INTRODUCTION

Nuclear magnetic resonance (NMR) spin lattice relaxation time (T_1) measurements in high resolution NMR spectra have become experimentally routine, both for small molecules and more recently for biomacromolecules. The great interest for proteins is the large amount of information about the motion of the protein, both overall and internal, which is potentially available from T_1 measurements. The nuclei most commonly studied are ^1H and ^{13}C , with recent interest in ^{19}F , ^{31}P , ^{15}N , and ^2D . The focus of this paper will be ^1H T_1 measurements. They are the easiest to accomplish because of the high sensitivity of ^1H NMR and they are potentially very valuable, given the large number of assigned ^1H NMR spectra of proteins.

The interpretation of ^1H T_1 measurements in proteins is not necessarily straightforward, however. The first and most obvious problem is that the T_1 's measured for many proteins, or for many different resonances in the spectrum of a particular protein,

Dr. Hull's present address is: Bruker-Physik AG, D-7512 Rheinstetten, Biberach, West Germany. Dr. Snyder's present address is: Department of Biochemistry, Stanford University School of Medicine, Stanford, Calif. 94305.

are all very nearly equal. They do not reflect the wide range of internuclear distances, internal motions, and overall rotational motions which would be expected. An example is the well characterized ^1H NMR spectrum of the bovine pancreatic trypsin inhibitor (BPTI) (1). At 100 MHz the measured T_1 's for the aromatic tyrosine and phenylalanine protons are all near 0.3 s. Similarly, at 270 MHz, the T_1 's are near 1.3–1.4 s and at 360 MHz the T_1 's are all near 1.5–1.6 s. The expected T_1 's for the aromatic protons, calculated from the X-ray structure of BPTI, should vary by more than a factor of three because of different internuclear distances, assuming in the calculation that internal motion of the tyrosines is not fast enough to influence relaxation. Also the calculated T_1 's predict a stronger field dependence than actually observed. Of course, if internal motion is fast enough to influence relaxation ($\tau_{\text{INT}} \lesssim 10^{-9}$ s), the calculated T_1 's will change (and the variation with field will diminish), but it seems unlikely that the differences in internal motions would so closely cancel out the effect of differences in internuclear distances. Alternatively, one could propose a more general overall mode of fast internal motion for the protein where the closest approach internuclear contacts are the same for all the protons on the protein and are modulated at the same rate. This also is not easily acceptable for the relatively rigid BPTI molecule.

Recently, it has been suggested for ^1H NMR on phospholipids (2), water in protein crystals (3), and hydrated collagen (4) that cross-relaxation can strongly influence and even dominate T_1 measurements. For proteins this has recently been put into focus by Kalk and Berendsen (5). The purpose of this paper is to present further experimental evidence bearing upon the role of cross-relaxation in ^1H T_1 measurements in proteins. Recent ^{19}F NMR measurements (6, 7) also provide evidence for the role of cross-relaxation in protein heteronuclear spin systems.

THEORY

NMR spin lattice relaxation in multispin systems is most generally expressed by a set of simultaneous differential equations. For a less abundant spin (S) such as ^{13}C or ^{19}F in the presence of a "bath" of abundant spins (I) such as ^1H 's in a protein, these equations can be written in the following fashion, with the nomenclature and assumptions of Hull and Sykes (6).

$$\begin{aligned} d[S_z]/dt &= -(\rho^{SI} + \rho^*)[S_z - S_0] - \sum_k \sigma_k^{SI}[I_z^k - I_0^k], \\ d[I_z]/dt &= -\sigma^{IS}[S_z - S_0] - \sum_k (\rho_k^{IS} + \rho_k^{II} + \sigma_k^{II})[I_z^k - I_0^k], \end{aligned} \quad (1)$$

where the summation is over all the abundant spins, k , and ρ^* represents relaxation mechanisms other than dipolar interactions with the abundant spins I .

The spin relaxation of the dilute S spins is simplified under two circumstances. The first, most common for ^{13}C , is when the abundant ^1H spins are saturated by double resonance irradiation during the ^{13}C T_1 measurement. Under these conditions

$[I_z^k]$ can be set equal to zero. Eq. 1 then simplifies to

$$d[S_z]/dt = (1/T_1)[S_z - (1 + \eta)S_0], \quad (2)$$

where $1/T_1 \equiv \rho^{SI} + \rho^*$ and the nuclear Overhauser enhancement

$$\eta \equiv \sum_k \sigma_k^{SI} I_z^k / (\rho^{SI} + \rho^*) S_0 = \left(\sum_k \sigma_k^{SI} / \sum_k \sigma_k^{SI} + \rho^* \right) (\gamma_I / \gamma_S). \quad (3)$$

For ^{19}F NMR measurements of proteins, the nuclear Overhauser enhancement upon ^1H decoupling is unfavorable (6) ($\eta \approx -1$). However, in the absence of decoupling, a simplification of Eq. 1 still exists from the fact that the ^1H "bath" is large (see Hull and Sykes [6]) and therefore I_z never deviates significantly from I_0 during the experiment. Under these circumstances Eq. 1 becomes

$$d[S_z]/dt = (-1/T_1)[S_z - S_0] \quad (4)$$

directly where $1/T_1 = \rho^{SI} + \rho^*$.

The situation for the ^1H T_1 relaxation time measurements is not so straightforward, however. This is most easily visualized by rewriting Eqs. 1 with the nomenclature of Kalk and Berendsen (5):

$$d[I_{zi}]/dt = -R_{ii}(I_{zi} - I_{0i}) - \sum_j R_{ij}(I_{zi} - I_{zj}), \quad (5)$$

where

$$R_{ii} = (3/10)\gamma^2\hbar^2 \sum_j (1/r_{ij}^6)[\tau_c/[1 + (\omega_0\tau_c)^2] + 4\tau_c/[1 + (2\omega_0\tau_c)^2]], \quad (6)$$

and

$$R_{ij} = \frac{1}{10} \frac{\gamma^4\hbar^2}{r_{ij}^6} \left[\tau_c - \frac{6\tau_c}{1 + (2\omega_0\tau_c)^2} \right]. \quad (7)$$

Here the presence of any dilute spins is neglected. The form of Eq. 5 is such that, if all of the ^1H 's are initially prepared in an equal nonequilibrium state such as after a nonselective 180° pulse, the resulting return to equilibrium will be as follows. Initially, when $I_{zi} = I_{zj} = -I_0$ and therefore $I_{zi} - I_{zj} = 0$, the relaxation will be single-exponential with time constant R_{ii} for each resonance i . At later times, however, if R_{ij} is large and positive, the second term in Eq. 5 will tend to keep I_{zi} and I_{zj} equal and force all resonances to relax with the same relaxation rate equal to the weighted sum of the individual relaxation rates. R_{ij} will be large for larger proteins with longer τ_c 's and at higher frequencies ω_0 .

Kalk and Berendsen (5) further propose that the protons in a protein can be divided roughly into three classes: (a) protons on aromatic residues and staggered aliphatic chains separated from each other by approximately 2.5 \AA and not moving internally in the protein fast enough to influence the nuclear spin relaxation (i.e., $\tau_{\text{INT}} \gg \tau_c$) (b) protons on CH_2 groups separated by approximately 1.8 \AA and also with no rapid internal motions and (c) protons on methyl groups, which will account for a large frac-

tion of the protons of a protein, and for which rapid internal motion about the methyl group axis is possible. With the further stipulation that for the purposes of cross-relaxation no proton is likely to be more than 2.5 Å away from another, the problems discussed in the introduction relative to the interpretation of ^1H spin-lattice relaxation times of proteins can be understood (see below).

METHODS:

Relaxation times at 100 MHz were measured with a Varian XL-100 NMR spectrometer (Varian Associates, Palo Alto, Calif.). Spin lattice relaxation times T_1 were determined using an inversion-recovery $(T-180-\tau-90)_N$ pulse sequence. Spin-spin relaxation time measurements were determined using a two-pulse spin echo pulse sequence $(T-90-\tau-180-\tau)_N$. Relaxation time measurements at 270 MHz and 360 MHz were measured with Bruker HXS-270 and HXS-360 NMR spectrometers (Bruker Instruments, Inc., Billerica, Mass.). All solutions were in D_2O and at 30°C.

The following conditions describe the preparation of the protein solutions with the numbering corresponding to the measurements presented in Figs. 1 and 4.

1. Bovine pancreatic trypsin inhibitor (mol wt ~ 6500) was obtained as a gift from Farbenfabriken Bayer AG (Elberfeld, W. Germany). The solution was 20 mg/ml in diethylamine buffer, pH 12.
2. Lysozyme (mol wt $\sim 14,400$) was obtained from P-L Biochemicals Inc. (Milwaukee, Wis.) (three times crystallized). The solution was 25 mg/ml, 10 mM citrate buffer, pH 4.52.
3. Trypsin (mol wt $\sim 23,800$) was obtained from Worthington Biochemical Corp. (Freehold, N.J.). The solution was 20 mg/ml, 10 mM Tris buffer, pH 8.1, 0.1 M NaCl.
4. α -chymotrypsin (mol wt $\sim 24,500$) was obtained from Worthington Biochemical Corp. The solution was 24 mg/ml, 10 mM potassium phosphate buffer, pH 7.8, 0.5 mM EDTA.
5. Ovalbumin (mol wt $\sim 45,000$) was obtained from Sigma Chemical Co. (St. Louis, Mo.). The solution was 20 mg/ml, 10 mM potassium phosphate buffer, pH 7.0, 0.5 mM EDTA.
6. Concanavalin A (mol wt $\approx 55,000$) was obtained as a gift from John Grimaldi (Harvard University, Cambridge, Mass.) (8). The solution was 20 mg/ml, 0.1 M acetate buffer, pH 5.35, 0.3 M NaCl.
7. Human serum albumin (mol wt $\sim 65,000$) was obtained from Sigma Chemical Co. The solution was 21 mg/ml, 10 mM potassium phosphate buffer, pH 7.0, 0.5 mM EDTA.
8. Oxyhemoglobin (mol wt $\sim 68,000$) was obtained from B. Manuck (Harvard University, Cambridge, Mass.) (9). The solution was 5 mg/ml 15 mM potassium phosphate buffer, pH 7.25.
9. Fluorotyrosine alkaline phosphatase from *E. coli* (mol wt $\sim 86,000$) was obtained from H. Weingarten and M. Schlesinger (Washington University, St. Louis, Mo.) (10). The solution was 26 mg/ml in 0.5 M Tris buffer, pH 7.9.
10. Aspartate transcarbamylase (catalytic subunit mol wt $\sim 100,000$) prepared as described by Rosenbusch and Weber (11) was obtained from T. Marinetti (Harvard University, Cambridge, Mass.). The solution was 45 mg/ml, 40 mM imidazole acetate buffer, pH 7.0, 0.4 mM EDTA, 5 mM β -mercaptoethanol.
11. Yeast alcohol dehydrogenase (mol wt $\sim 150,000$) was obtained from Sigma Chemical Co. The solution was 25 mg/ml, 10 mM potassium phosphate buffer, pH 7.10, 0.5 mM EDTA.

RESULTS AND DISCUSSION

The relaxation time $T_1 = 1/R_{1i}$ calculated for the three classes of protons a, b, and c at 100 MHz are shown by the respective curves A, B, and C in Fig. 1. These

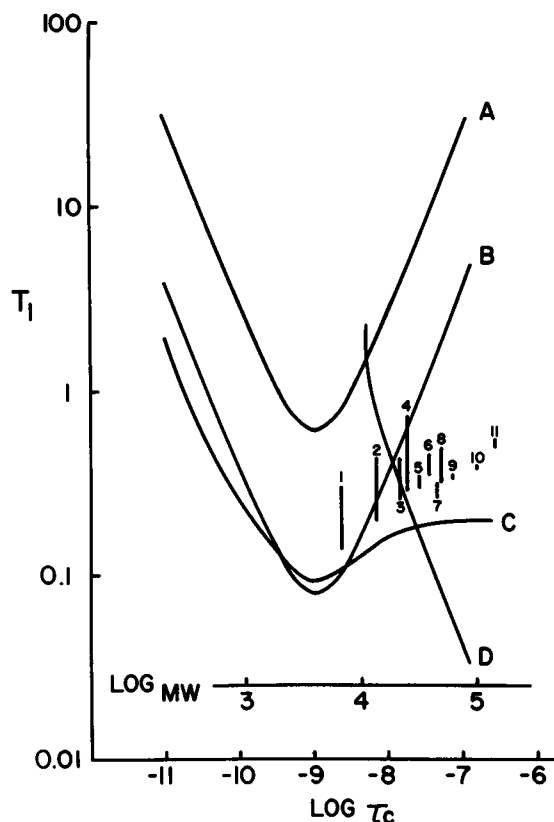


FIGURE 1 Calculated relaxation times ($1/R_H$ from Eq. 6) at 100 MHz are presented in curve *A* for r_{ij} 2.5 Å, and in curve *B* for r_{ij} 1.78 Å, as a function of the rotational correlation time τ_c . Curve *C* is the calculated relaxation time for a CH_3 group (r_{ij} 1.78 Å) as a function of the rotational correlation time τ_c with a correlation time for internal motion $\tau_{\text{INT}} 5 \times 10^{-10}$ s (5,15). Curve *D* is the relaxation time corresponding to cross-relaxation ($1/R_{ij}$) calculated from Eq. 7 as a function of the rotational correlation time τ_c for r_{ij} 2.5 Å. The vertical lines represent the range of experimental measured relaxation times for the following proteins: 1, bovine pancreatic trypsin inhibitor; 2, lysozyme; 3, trypsin; 4, α -chymotrypsin; 5, ovalbumin; 6, concanavalin A; 7, human serum albumin; 8, oxyhemoglobin; 9, alkaline phosphatase; 10, aspartate transcarbamylase catalytic subunit; 11, yeast alcohol dehydrogenase. See Methods for details of the individual solutions. The range of measured relaxation times is positioned above the appropriate τ_c for the corresponding molecular weight. T_1 's and τ_c 's are in units of seconds.

are identical to the calculations of Kalk and Berendsen (5), with the exception that the methyl group rotation is assumed to be diffusional with a τ_{INT} chosen equal to 5×10^{-10} s for this calculation. Other values of τ_{INT} produce a family of similarly shaped curves but lying mostly above curve *C* for $\tau_c \geq 10^{-8}$ s. As can be seen quite clearly from Fig. 1, the time constant for the cross-relaxation (curve *D*) becomes much shorter than any of the other relaxation rates for τ_c longer than 10^{-8} s. For higher frequencies ω_0 , this will occur for smaller τ_c 's.

Also appearing in Fig. 1 is a second scale, corresponding to protein molecular

weight, positioned above the scale corresponding to rotational correlation time τ_c , in such a manner that the protein molecular weight is matched to the appropriate rotational correlation time for a protein of that size. This was determined from a survey of measured rotational correlation times for proteins by fluorescence depolarization and ^{13}C NMR (W.E. Hull, unpublished results). It also matches reasonably well the rotational correlation times calculated from the Stokes-Einstein equation. The numbered vertical bars then represent the experimentally measured range of relaxation times T_1 measured at a variety of positions in the ^1H NMR spectrum of the several proteins at 100 MHz. Each protein was measured under conditions of no aggregation and the experimental range of T_1 values is positioned relative to the molecular weight axis. One possible exception is BPTI where ^{13}C NMR T_1 measurements have determined a longer τ_c than expected on the basis of its molecular weight although the protein concentrations were higher than in the ^1H NMR experiments (12).

Several conclusions can be made. First, the measured range of relaxation times falls between the limiting values calculated *a priori* for the various classes of protons. Secondly, the range of values of T_1 measured decreases markedly for the larger proteins, in a molecular weight (τ_c) range where cross-relaxation would be expected to have a greater role in the relaxation, causing all of the protons to relax with the same

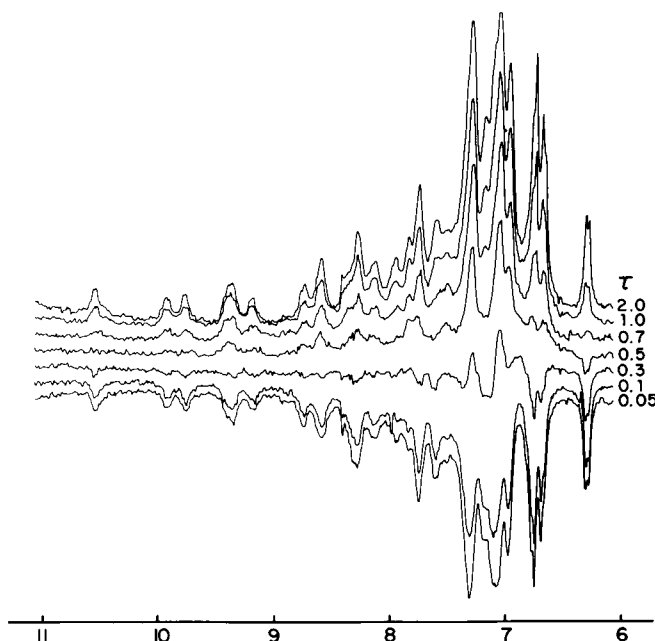


FIGURE 2 270 MHz T -180- τ -90 inversion-recovery spin lattice relaxation time measurements for the bovine pancreatic trypsin inhibitor. The solution was unbuffered pH 6. Only the aromatic and NH regions of the spectrum are shown. Detailed assignments are available elsewhere (1). The chemical shift scale is in parts per million downfield from DSS. The long τ value spectra are not shown. τ values are in units of seconds.

weighted average relaxation rate. Thirdly, the behavior of the relaxation times measured as a function of molecular weight follows curve C, as would be expected if the predominant, fast-relaxing methyl groups dominate the averaged relaxation rate. Therefore the simple phenomenological model for proteins (5) described above correctly predicts the features of the experimental T_1 measurements as a function of molecular weight. Of course, the spectra of the larger proteins at 100 MHz are more unresolved envelopes than resolved resonances. However, no faster or slower relaxing components were observed in any region of the spectrum.

The second form of experimental verification is shown in Fig. 2 and 3. Fig. 2 shows 270 MHz ^1H NMR inversion-recovery T_1 measurements on the small bovine pancreatic

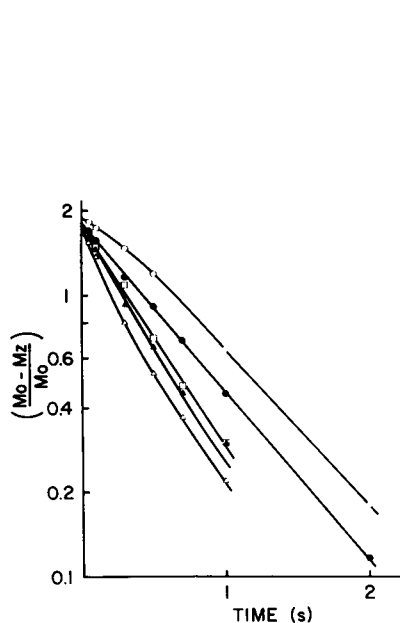


FIGURE 3

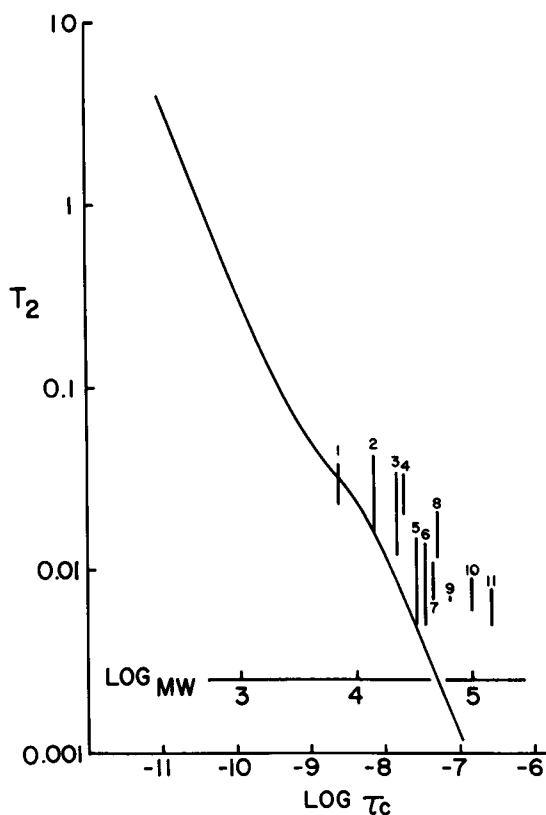


FIGURE 4

FIGURE 3 Semilogarithmic plots of the 270 MHz inversion-recovery relaxation time measurements shown in part in Fig. 2. Tyr 23 3,5 protons at $\delta 6.35$ (○); Tyr 21 2,6 protons at $\delta 6.7$ (●); NH proton at $\delta 9.3$ (□); Phe protons at $\delta 7.3$ (▲); CH_3 protons at $\delta 0.7$ (△).

FIGURE 4 Calculated values of T_2 from Eq. 8 ($r_H = 1.78 \text{ \AA}$) as a function of the rotational correlation time τ_c are represented by a solid curve. The numbered vertical lines represent the range of experimentally measured values of T_2 determined for the proteins listed in the legend for Fig. 1, positioned above the appropriate τ_c corresponding to their molecular weight. T_2 and τ_c values are in units of seconds.

trypsin inhibitor protein. The assignment of the features of this spectrum are described elsewhere in detail (1). In this small protein (see discussion of τ_c above), differential relaxation behavior would be expected as discussed in the introduction and can be observed by careful measurements at the higher fields where the relaxation times are longer and more easily distinguished experimentally. For example, the Tyr 23 3,5 protons at 6.35 ppm downfield from DSS relax more slowly than the Tyr 21 protons at 6.7–6.8 ppm. However, as shown in Fig. 3, the relaxation of these resonances does not follow a single exponential. The slowest relaxing Tyr 23 protons begin to catch up in relaxation rate to the fastest relaxing CH₃ protons, which, in turn, tend to slow down in relaxation rate. This is an example of a cross-relaxation situation where the intrinsic relaxation rates (R_{ii}) and the cross-relaxation rate (R_{ij}) are about equal.

The measurement of T_2 is not similarly influenced by cross-relaxation (13). Each resonance can be characterized by a line width or spin-spin relaxation time T_2 . Fig. 4 shows a calculation of T_2 as a function of rotational correlation time τ_c (or molecular weight):

$$1/T_2 = (3/20)\gamma^4\hbar^2 \sum_{ij} (1/r_{ij}^6)[3\tau_c + 5\tau_c/[1 + (\omega_0\tau_c)^2] + 2\tau_c/[1 + (2\omega_0\tau_c)^2]] \quad (8)$$

The solid curve is for no internal motion and $r = 1.78 \text{ \AA}$. For all other cases within a protein, such as longer distances or internal motion, the value of T_2 will lie above the curve shown. The experimental values, determined for the same proteins as Fig. 1 and also at 100 MHz, fall above the calculated curve with the shortest values lying on or near the curve. (Deviations at the higher molecular weights may reflect an inability to measure the correspondingly short T_2 's.) The range of values measured does not appreciably diminish with increasing molecular weight. How much internal motion might be present can be estimated (14) by considering that very rapid internal motion ($\tau_{\text{INT}} \lesssim 10^{-11} \text{ s}$) about an axis making an angle θ with the internuclear vector of interest reduces the line width by $[(3 \cos^2 \theta - 1)/2]^2$. For CH₃ groups ($\theta = 90^\circ$) the line width is reduced by $\frac{1}{4}$.

CONCLUSION

The experimental evidence presented in this manuscript has been interpreted in terms of the theory of Kalk and Berendsen and supports the conclusion that cross-relaxation can play an important role in the ¹H spin lattice relaxation in proteins. In fact, cross-relaxation clearly can dominate the relaxation of larger proteins even at relatively low resonance frequencies. This means that ¹H T_1 measurements are not so straightforward a measure of either differential motion or differential internuclear contact within a protein.

Undoubtedly, internal motions of an intermediate-to-fast rate ($10^8 - 10^{10} \text{ s}^{-1}$) are involved in proteins, some much more than others. These motions will reduce the effectiveness of cross-relaxation by decreasing the rate R_{ij} while increasing R_{ii} . The interplay between these motions and cross-relaxation will make it difficult, in general,

to sort out the contribution of each to the relaxation. Also magnetically isolated regions of the protein (such as surface histidine C2 proteins), proteins relatively devoid of methyl groups (such as collagen), or a distribution of correlation times for some systems (16) are possible.

These reservations notwithstanding, the Kalk and Berendsen theory accounts for all of the qualitative aspects of the measured T_1 's presented in this manuscript and cautions against the interpretation of any ^1H T_1 measurements in large proteins in terms of internal motions without consideration of the magnitude of the cross-relaxation effects. In fact, even in simple spin systems and smaller molecules the effects of cross-relaxation can be seen (17). The influence on the relaxation curves is in the opposite direction, however, reflecting a change in sign of R_{ij} . Also the magnitude of R_{ij} cannot exceed or even equal that of R_H in the case of smaller molecules.

Received for publication 5 August 1977 and in revised form 25 October 1977.

REFERENCES

1. SNYDER, G. H., R. ROWAN III, S. KARPLUS, and B. D. SYKES. 1975. Complete tyrosine assignments in the high field ^1H nuclear magnetic resonance spectrum of the bovine pancreatic trypsin inhibitor. *Biochemistry*. **14**:3765-3777.
2. SEITER, C. H. A., and S. I. CHAN. 1973. Molecular motion in lipid bilayers. A nuclear magnetic resonance linewidth study. *J. Am. Chem. Soc.* **95**:7541-7553.
3. HSI, E., and R. G. BRYANT. 1977. Dynamic problems at the water-protein interface: results from NMR relaxation. *Biophys. J.* **17**:54a. (Abstr.).
4. EDZES, H. T., and E. T. SAMULSKI. 1977. Cross relaxation and spin diffusion in the proton NMR of hydrated collagen. *Nature (Lond.)*. **265**:521-523.
5. KALK, A., and H. J. C. BERENDSEN. 1976. Proton magnetic relaxation and spin diffusion in proteins. *J. Magn. Resonance*. **24**:343-366.
6. HULL, W. E., and B. D. SYKES. 1975. Dipolar nuclear spin relaxation of ^{19}F in multispin systems. Application to ^{19}F labelled proteins. *J. Chem. Phys.* 1975. **63**:867-880.
7. HULL, W. E., and B. D. SYKES. 1975. Fluorotyrosine alkaline phosphatase: internal mobility of individual tyrosines and the role of chemical shift anisotropy as a ^{19}F nuclear spin relaxation mechanism in proteins. *J. Mol. Biol.* **98**:121-153.
8. GRIMALDI, J. J., and B. D. SYKES. 1975. Concanavalin A: a stopped flow nuclear magnetic resonance study of conformational changes induced by Mn^{++} , Ca^{++} , and α -methyl-D-mannoside. *J. Biol. Chem.* **250**:1618-1624.
9. MANUCK, B. A., J. G. MALONEY, and B. D. SYKES. 1973. Kinetics of the interaction of methyl isonitrile with hemoglobin β chains: measurement by nuclear magnetic resonance. *J. Mol. Biol.* **81**:199-205.
10. SYKES, B. D., H. I. WEINGARTEN, and M. J. SCHLESINGER. 1974. Fluorotyrosine alkaline phosphatase from *Escherichia coli*: preparation, properties, and fluorine-19 nuclear magnetic resonance spectrum. *Proc. Natl. Acad. Sci. U.S.A.* **71**:469-473.
11. ROSENBUSCH, J. P., and K. WEBER. 1971. Subunit structure of aspartate transcarbamylase from *Escherichia coli*. *J. Biol. Chem.* **246**:1644-1657.
12. WÜTHRICH, K. 1976. NMR in biological research. Elsevier North-Holland, Inc., New York. 217-218.
13. ABRAGAM, A. 1961. Principles of Nuclear Magnetism. Oxford University Press.
14. MARSHALL, A. G., P. G. SCHMIDT, and B. D. SYKES. 1972. Effect of internal rotation on nuclear magnetic relaxation times for macromolecules. *Biochemistry*. **11**:3875-3879.
15. WOESSNER, D. E. 1962. Spin relaxation processes in a two-proton system undergoing anisotropic re-orientation. *J. Chem. Phys.* **36**:1-4.

16. TORCHIA, D. A., J. R. LYERLA, and A. J. QUATTRONE. 1975. Molecular dynamics and structure of the random coil and helical states of the collagen peptide, $\alpha 1$ -CB2, as determined by ^{13}C magnetic resonance. *Biochemistry*. **14**:887-900.
17. CAMPBELL, I. D., and R. FREEMAN. 1973. Influence of cross relaxation on NMR spin-lattice relaxation times. *J. Magn. Resonance*. **11**:143-162.